High-Performance Adaptive Perturb and Observe MPPT Technique for Photovoltaic-Based Microgrids

Ahmed K. Abdelsalam, *Member, IEEE*, Ahmed M. Massoud, *Member, IEEE*, Shehab Ahmed, *Member, IEEE*, and Prasad N. Enjeti, *Fellow, IEEE*

***Abstract*—Solar photovoltaic (PV) energy has witnessed double-digit growth in the past decade. The penetration of PV systems as distributed generators in low-voltage grids has also seen significant attention. In addition, the need for higher overall grid efficiency and reliability has boosted the interest in the microgrid concept. High-efficiency PV-based microgrids require maximum power point tracking (MPPT) controllers to maximize the harvested energy due to the nonlinearity in PV module characteristics. Perturb and observe (P&O) techniques, although thoroughly investigated in previous research, still suffer from several disadvantages, such as sustained oscillation around the MPP, fast tracking versus oscillation tradeoffs, and user predefined constants. In this paper, a modified P&O MPPT technique, applicable for PV systems, is presented. The proposed technique achieves: first, adaptive tracking; second, no steady-state oscillations around the MPP; and lastly, no need for predefined system-dependent constants, hence provides a generic design core. A design example is presented by experimental implementation of the proposed technique. Practical results for the implemented setup at different irradiance levels are illustrated to validate the proposed technique.**

***Index Terms*—Maximum power point tracking (MPPT), perturb and observe (P&O), photovoltaic (PV).**

I. Introduction

MICROGRID, a recently emerging power technology, is expected to possess an increasing role in future power systems due to its immense advantages. The need for more flexible electricity systems, energy savings, and environmental impact are driving the development of microgrids. The microgrid concept has been proposed as a solution to the conundrum of integrating several power generations without disturbing the utility, especially when renewable energy sources are utilized [1]–[3].

Renewable energy sources involve many aspects: efficiency, reliability, cost, safe connection to the electric grid, capability to manage microgrids, energy storage, low environmental impact, and development of advanced control and monitoring algorithms [4]. The most common renewable energy sources are hydroelectric, photovoltaic (PV), and wind. Despite that hydroelectric energy production is the dominant, the PV energy sector is growing at more than 30% per year [4]. Connecting multiple of these sources to the utility introduces varying dynamics. As PV sources are intermittent, nonlinear, and produce power that varies with environmental conditions, an adequate maximum power point tracking (MPPT) is needed [4], [5].

The nonlinear characteristic of a PV panel is a function of irradiance and temperature, as shown in Fig. 1. For best utilization of the available energy, it is necessary to operate the system at its MPP. Several techniques have been proposed for maximum power tracking [5]–[7]. Among them, the perturb and observe (P&O) method is the most common for simplicity, ease of implementation, and good performance [5], [6]. Many researches investigate the PV array nonlinear behavior [8] and associated grid-connected inverters [9], [10].

It is reported that P&O techniques suffer several demerits [5]–[7]. For fixed perturb values, the steady-state oscillations are proportional to the perturb value. Large perturb values cause higher oscillation. Unfortunately, smaller perturb values result in slower response. Hence, the famous tradeoff problem between faster response and steady-state oscillations is inherent. Moreover, the perturb value is not generic, therefore, MPPT using a fixed perturb is system dependent [11]–[33].

For improved performance, a variable perturb is utilized. Initial attempts use varying perturb values dependent on output power. Although these techniques are not truly adaptive, yet they present improved performance relative to their fixed perturb counterparts [34]–[36]. Other techniques propose truly adaptive modifications, but suffer from a high computational load due to aggressive derivatives [37], [40] and need initial user-dependent constants for the perturb adaptation [38], [39]. Novel techniques show improved performance using nonlinear equations [41], fuzzy logic [42], and complicated optimization algorithms [43], [44], yet not common due to their complexity and need of sophisticated controllers [5]–[7].

In this paper, an innovative P&O technique is presented. The proposed technique utilizes the rate of change of the array power and treats it by a proportional-integral (PI)-controller to generate an adaptive perturb. Advantages of the proposed technique are as follows:

1) an adaptive algorithm that varies the perturb value automatically according to the system changes;
2) simple to implement as only a PI-controller is needed;
3) no oscillation during tracking and steady-state operations;
4) low computational burden required, hence, fast tracking using low-cost controllers is achievable;

Manuscript received June 29, 2010; revised October 4, 2010; accepted December 31, 2010. Date of current version June 10, 2011. Recommended for publication by Associate Editor H. Akagi.

A. K. Abdelsalam, S. Ahmed, and P. N. Enjeti are with the Department of Electrical and Computer Engineering, Texas A&M University at Qatar, Doha 23874, Qatar (e-mail: ahmed.abdel-salam@qatar.tamu.edu; shehab.ahmed@qatar.tamu.edu; prasad.enjeti@qatar.tamu.edu).

A. M. Massoud is with the Department of Electrical Engineering, Faculty of Engineering, Qatar University, Doha 2713, Qatar (e-mail: ahmed.massoud@qu.edu.qa).

Color versions of one or more of the figures in this paper are available online at http://ieeexplore.ieee.org.

Digital Object Identifier 10.1109/TPEL.2011.2106221

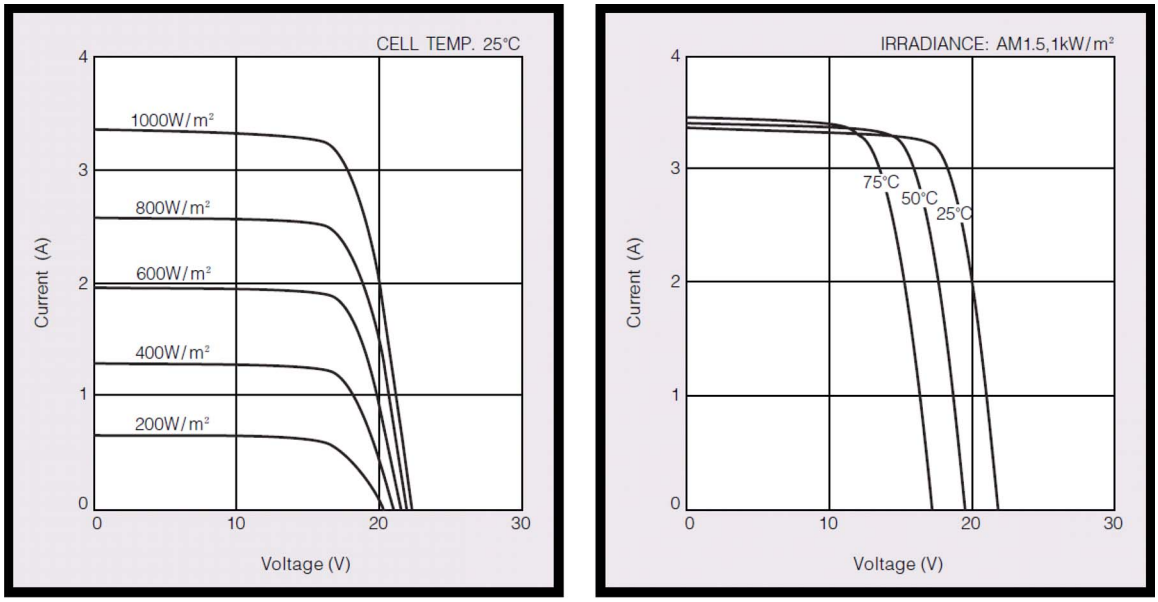

(a) (b)

Fig. 1. Typical PV array nonlinear characteristics, KYOCERA KC50T PV array [46]. (a) Variation of PV array characteristics with solar irradiance, temperature is fixed at 25 °C. (b) Variation of PV array characteristics with temperature, irradiance is fixed at 1000 W/m^2.

5) No preset constants are needed.

The paper is organized in five sections. Following the introduction in Section I, a detailed survey of over 35 journal/conference published technical papers related to P&O techniques is illustrated in Section II. The proposed adaptive P&O technique, named PI-P&O, is discussed in Section III. In Section IV, the experimental setup is addressed with practical results to validate the advantages of the proposed technique. Finally, a conclusion is given in Section V.

II. P&O Techniques Survey

As shown in Fig. 2, P&O techniques can be classified into five groups according to the controlled variable output from MPPT block and the perturb value generation method. The following sections discuss previous research regarding these techniques.

A. Conventional P&O With Fixed Perturb

Research belonging to this group is the backbone of the P&O techniques. In this method, a fixed perturb value is utilized to generate a reference signal for the outer control loop. The perturb signal is either the array reference voltage or current. The fixed perturb step is determined according to the system designer as a result of previous experience. Therefore, the solution provided by this method is not generic and system dependent. For small perturb steps, the tracking is slow but the power/voltage oscillations are minimal. In the case of large perturb step, faster tracking is achieved with increased oscillations. Hence, P&O techniques with fixed perturb suffer an inherent tracking–oscillations tradeoff problem. A PI/hysteresis controller following the MPPT is utilized to control the power converter. A review of research related to this technique is illustrated in Table I.

B. Modified P&O With Fixed Perturb

In this technique, instead of utilizing the array voltage or current as the perturbed signal, the converter duty ratio is used. This eases the control process as it eliminates the PI/hysteresis controller after the MPPT block, enabling direct control of the converter's duty cycle. Like group A, the perturb step is fixed and designer dependent. Hence, the previously mentioned tradeoff problem still persists. Table II shows previous research associated with this technique.

In order to improve the performance of P&O techniques, the adaptive calculation of the perturb value is utilized instead of the fixed values used in groups A and B. The adaptive P&O techniques review are discussed in the following sections.

C. Conventional P&O With Adaptive Perturb

Al-Amoudi *et al*. [34] proposed a method to vary the perturb value during the hill climbing process. Initially, the voltage perturb is set to be 10% of the open-circuit voltage. Each successive perturb is 50% of the previous one until the perturb value is 0.5% of the open-circuit voltage. Despite the acceptable results this method shows, it is still not fully adaptive as the perturb steps are predetermined. Moreover, it depends on the open-circuit voltage, which varies with the environmental conditions. The method was verified on a grid-connected three-phase single-stage inverter. A similar method using a model-based approach to determine the PV array voltage and current from the irradiance and temperature was introduced by Zehang *et al.* [35]. Patel and Agarwal [36] proposed a variable perturb by adopting

TABLE I
CONVENTIONAL P&O WITH FIXED PERTURB FROM RESEARCH SURVEY

Ref.	*Authors*	*Publication year*	*MPPT output variable*	*Converter control technique*	*Converter type, Application*	*Controller implementation*	*NOTES*
[11]	O.Wasynezuk	1983	V_{pv}^{*}	PI	Single phase single stage full bridge converter with line frequency transformer, grid connection	Analog electronics	Poor tracking in case of rapid changing weather
[12]	W. Teulings *et al.*	1993	V_{pv}^{*}	PI	Buck-boost converter for battery charge/discharge and buck converter for fixed DC voltage loads, space application	Mixed analog and digital electronics	Changing weather is not deeply considered in space applications
[13]	C. Hua *et al.*	1996	V_{pv}^{*}	PI	Buck converter, battery load	Microcontroller *TMS320C25*	Improve tracking performance in rapidly changing weather by increase execution time
[14]	Y. Kim *et al.*	1996	I_{pv}^{*}	Hysteresis	Boost converter, battery load	Mixed analog and digital electronics	Reduced cost and simple implementation
[15]	Y. Jung *et al.*	2002	I_{inv}^{*}	Hysteresis	Full bridge converter high frequency DC-link with high frequency transformer, rectification stage and single phase inverter, grid connection	Microcontroller *Kier board*	bulky nominal frequency isolation transformer replaced by high frequency DC-link
[16]	K. Chomsuwan *et al.*	2002	I_{pv}^{*}	PI	Two-switch buck-boost converter cascaded with unfolding full bridge single phase inverter, grid connection	Microcontroller *ADMC331*	Grid connection without isolated high frequency transformer and diode rectification stage
[17]	T. Shimizu *et al.*	2003	V_{pv}^{*}	PI	Novel multistage generation control circuit cascaded with half bridge single phase inverter, grid connection	Microcontroller -	Very good results in partial shading conditions
[18]	N. Femia *et al.*	2008	V_{pv}^{*}	PI	Distributed MPPT for boost converter, string array connection	-	Improved tracking in partial shading conditions
[19]	M. Fortunato *et al.*	2008	V_{pv}^{*}	PI	Single phase single stage full bridge converter with line filter, grid connection	Real time contol *NI Compact RIO 9004*	One cycle controller is designed with multi-objective for performance improvement under rapidly changing weather
[20]	E. Figueres *et al.*	2009	V_{pv}^{*}	PI	Three phase single stage VSI inverter, grid connection	Microcontroller *TMS320F2812*	Proposed accurate small-signal model of high-power grid-connected PV inverters with LCL Filter with detailed sensitivity analysis
[21]	H. Patel *et al.*	2010	V_{pv}^{*}	PI	Boost converter cascaded with single phase full bridge inverter, PV based active power filters	-	Multi-string and centralized inverter connections achieve better performance than series array configuration in partial shading conditions
[22]	S.-H. Park *et al.*	2010	V_{pv}^{*}	PI	Boost converter with simplified auxiliary resonance circuit	Microcontroller *ATMega128*	Improved efficiency and loss reduction due to all-switch zero-current turn-on and zero-voltage turn-off operation

TABLE II
MODIFIED P&O WITH FIXED PERTURB FROM RESEARCH SURVEY

Ref.	*Authors*	*Publication year*	*MPPT output variable*	*Converter type, Application*	*Controller implementation*	*NOTES*
[23]	M.Solnim *et al.*	1996	CSI firing angle	Single phase single stage CSI thyristor based with isolation line frequency transformer, grid connection	-	Initial compulsory perturb is mandatory
[24]	N. Kasa *et al.*	2000	d^{*}	Two stage two-switch buck-boost converters, grid connection	Microcontroller *TMS320C31*	MRAS is utilized to estimate capacitor value and correct the calculated duty ratio. No line frequency isolation transformer is used.
[25]	E. Koutroulis *et al.*	2001	d^{*}	Buck converter, battery load	Microcontroller *80C196*	15% increase in power due to MPPT compared to constant duty ration operation
[26]	M. Veerachary *et al.*	2001	d^{*}	Interleaved dual boost converter, battery load	PC+DAQ card	IDB converter reduces current ripples. MPPT utilize voltage sensor only as power calculation is considered to be dependent on the array voltage and the converter efficiency which is taken constant in this paper (neither verified nor proofed)
[27]	Y. Hsiao *et al.*	2002	d^{*}	Boost converter, resistive load	Microcontroller -	Compares three points, instead of two, to minimize oscillations
[28]	N. Kasa *et al.*	2005	d^{*}	Fly back inverter with center-tapped secondary winding, grid connection	Microcontroller *TMS320C31*	Current sensorless MPPT is proofed by estimating the array current from capacitor voltage, duty ratio and converter passive elements
[29]	S. Jain *et al.*	2007	d^{*}	Novel connected two buck-boost converters, grid connection	Microcontroller *TMS320LF2407*	Novel configuration for single phase single stage PV grid connected converters
[30]	R. Gules *et al.*	2008	d^{*}	Bi-directional two switch boost converter, battery load	Microcontroller *MSP430F149*	Parallel connected converter to decrease processed array power, hence decrease losses and achieve battery charging plus boosting operation
[31]	J. Kwon *et al.*	2008	d^{*}	Three level boost converter, grid connection	Microcontroller *dspic30F6015*	Utilizes previous array power to create power hysteresis to detect insolation changes. Modified duty cycle to balance the converter capacitors
[32]	J. Kwon *et al.*	2009	d^{*}	Multistring PV parallel boost converters, grid connection	Microcontroller *dspic30F3011*	Same as [28] with the addition of duty cycle update to reduce power oscillations in DC side due to single phase grid connection
[33]	C. Liu *et al.*	2010	d^{*}	SEPIC converter, grid connection	-	PV-wind hybrid generation system is proposed with grid connection

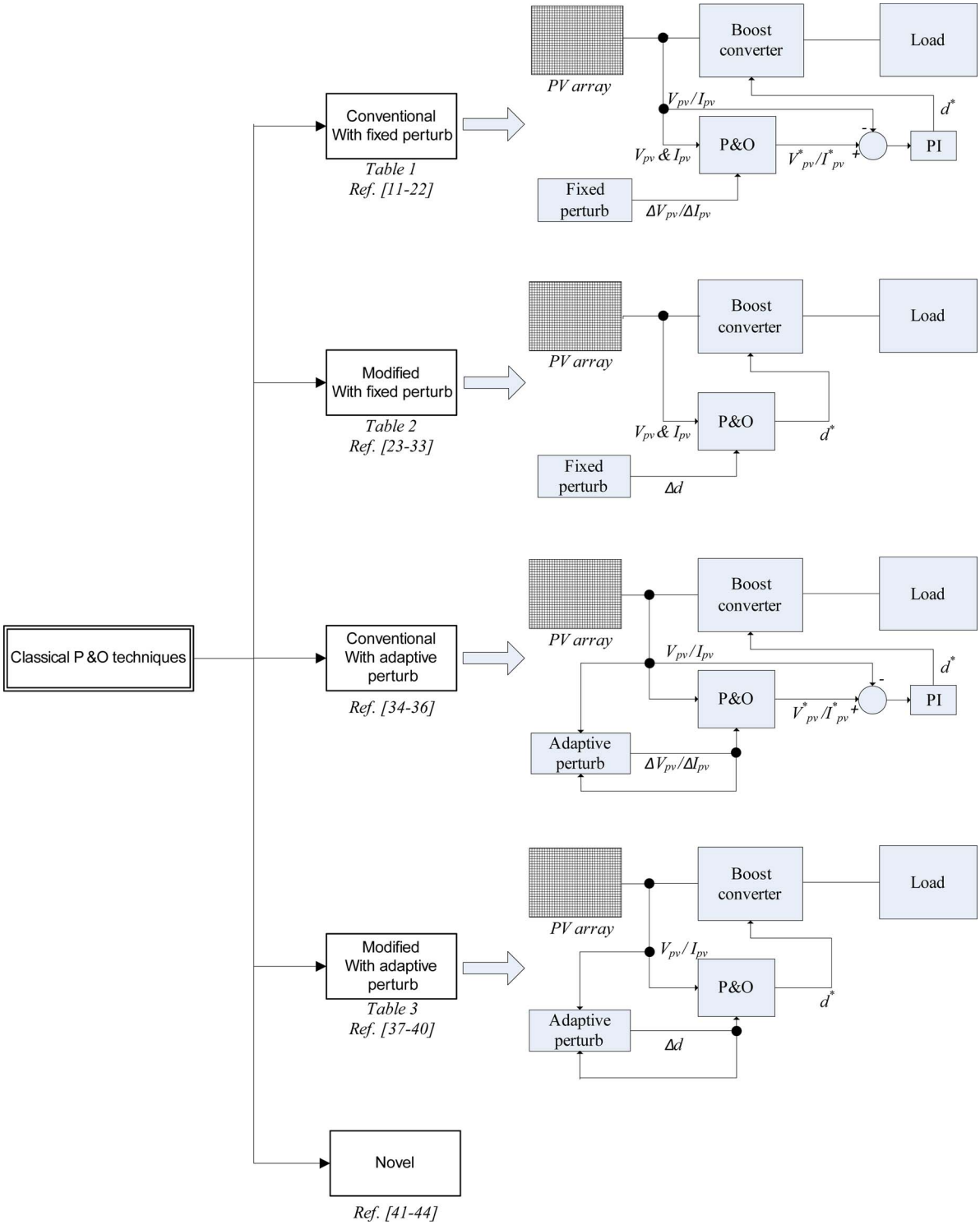

Fig. 2. P&O techniques classification.

four power ranges. In each range, a specific perturb value is used; hence, the method is not fully adaptive as well.

D. Modified P&O With Adaptive Perturb

Several attempts have been proposed to improve the performance of the modified P&O using adaptive perturb. Despite of good performance, these techniques suffer several demerits, such as high computational load versus accuracy tradeoff and predefined constants dependency. Details of these techniques are discussed in Table III.

E. Novel P&O With Fixed/Adaptive Perturb

Novel methods have been proposed to improve the P&O performance with sophisticated yet complicated algorithms. Jain

TABLE III
MODIFIED P&O WITH ADAPTIVE PERTURB FROM RESEARCH SURVEY

Ref.	*Authors*	*Publication year*	*Perturb*	*Converter type, Application*	*Controller implementation*	*NOTES*
[37]	M. Chiang *et al.*	2002	$d(k) = d(k-1) \pm \frac{\lvert\Delta P/\Delta d\rvert}{\lvert P/d\rvert}$	Boost converter, battery load	Microcontroller *TMS320F240*	High computational loads due to derivatives, high non linearity in P/d derivative term, true adaptive
[38]	W. Xiao *et al.*	2004	$d(k) = d(k-1) \pm \frac{M\lvert\Delta P\rvert}{d(k-1)}$	Buck converter, battery load	Microcontroller *TMS320LF2407*	Less computational load, constant M needs to be predefined, system design dependant, true adaptive
[39]	P. Wolf *et al.*	2005	$d(k) = d(k-1) + M\frac{dP}{dV}$	Buck converter, applied to cell level in vehicle solar array	Microcontroller *MSP430*	Less computational load, less non linearity in P/V derivative term, constant M needs to be predefined, system design dependant, true adaptive
[40]	A. Pandey *et al.*	2008	$d(k) = d(k-1) + M\frac{dP}{dV}$	Buck converter, battery load	Microcontroller *ADuC831*	More computational load, less non linearity in P/V derivative term, constant M is automatically calculated, works with full curve evaluation algorithm for power level detection, fully adaptive

and Agarwal [41] utilized nonlinear equations to get close to the MPP. The controlled variable is not the array power, yet a variable named β, which is a nonlinear function of the array voltage, current, and power. The new controlled variable gives a monotonically increasing relationship with the duty cycle. After getting close to the MPP, conventional P&O can be applied for fine tuning. Although good results were proven, the high computational load clearly complicates this technique.

D'souza *et al.* [42] proposed a fuzzy logic MPPT. Despite its improved performance, especially in partially shaded conditions, the method requires many parameters to be selected by the designer, such as the fuzzy sets, membership function, and rule base.

Femia *et al*. achieved improved tracking performance by optimizing the duty cycle and sampling rate of PV voltage/current [43]. Unfortunately, the optimization relies on customizing these parameters for a specific converter and PV array. Additionally, they proposed a compensation network, a transfer function affecting MPPT output signal, to minimize power oscillations in two-stage single-phase converter systems [44].

III. PROPOSED P&O TECHNIQUE

As discussed in the presented review, all attempts seek either sophisticated performance with the penalty of cost/complexity or moderate performance with acceptable cost and relative simplicity. Hence, the proposed P&O technique attempts to achieve improved performance with moderate cost, simple implementation, and a generic core that does not depend on preset constant values.

A. Theory

The block diagram of the proposed P&O technique is shown in Fig. 3. The main idea behind the proposed technique is that at the start of any hill climbing technique, large perturb steps are needed to quickly reach the MPP, and as the MPP is approached, the perturb value needs to be decreased to avoid large oscillations around this maximum output power operating point. As explained in Section II, P&O techniques, either conventional or modified, are not capable of achieving this target if the perturb value is fixed. Therefore, adaptive techniques are the only solutions.

The proposed adaptive technique utilizes the error between two successive array power signals calculated from the measured array voltage and current signals to create an adaptive perturb. Basically, at the start of the hill climbing process, this error is large and decreases as the maximum power operating point is approached at steady state. Therefore, this error can be treated like an error signal in a closed-loop system that needs to be minimized at steady state, prevented from overshoot at startup, and free from steady-state oscillations. The simplest clue to achieve all these targets is to treat this error signal using a conventional PI controller, which is the main core of the proposed technique. Hence the name PI–P&O technique is being proposed. This PI controller is utilized as the adaptive perturb value generator for the reference array voltage.

Another PI controller is used for the boost converter. Its function is to force the PV array input voltage to track the reference voltage from the MPPT block. The proposed system requires two signals to be measured: PV array voltage and current. Therefore, by tuning both PI controllers, good performance is achieved with less computational load and no predefined constants.

The boost converter is modulated at 25 KHz to minimize oscillations in the converter output voltage. The effect of this high switching frequency on switching losses is considered in the insulated gate bipolar transistor and fast diode selection. Also, the whole control algorithm runs at this sampling frequency. The measured array voltage and current are filtered using a low-pass filter tuned at 1000 Hz to mitigate any associated/picked-up noise on the measured signals. In order to generate two successive samples for the array power, a delay of 100 samples ($100 \times 40\ \mu$s) is used. This relatively long delay effect on the control algorithm is irrelevant due to the long time constant of the array power variation.

B. Mathematical Model and Governing Equations

This section describes the proposed technique's mathematical model, governing equations, and implementation steps. In order to briefly illustrate these targets simultaneously, the system equations are described in steps showing the controller implementation. Also, for more clarification, system equations

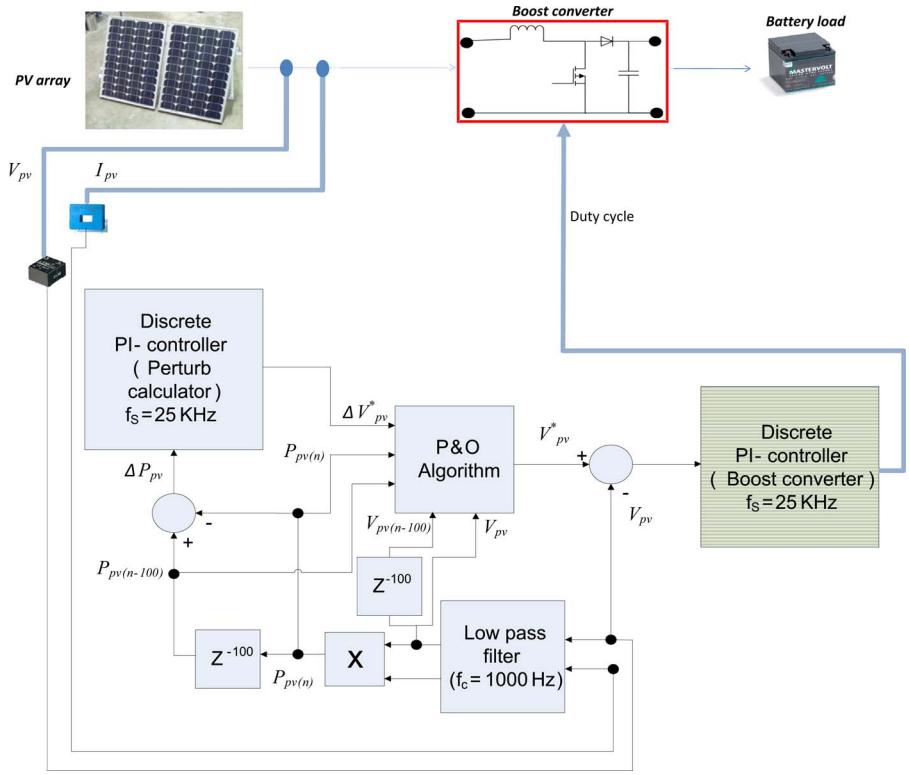

Fig. 3. Proposed P&O technique (PI–P&O).

are represented in a difference equation format to illustrate the system discretization and sampling time effect. The system principle of operation is as follows.

1) The first step is to read the PV array voltage $V_{\mathrm{PV}}(n)$ and current $I_{\mathrm{PV}}(n)$ signals, where n refers to the present sample instant.
2) For measurement noise reduction, the measured array voltage and current signals need to be filtered. A low-pass filter tuned at corner frequency $f_c = 1000$ Hz ($\tau_c = 15.9$ ms) is used, and the sampling frequency f_s is 25 KHz ($\Delta T_s = 40\ \mu$s), as stated in Section III-A.

$$V_{\mathrm{PV\_filtered}}(n) = [V_{\mathrm{PV\_filtered}}(n-1)][1-\alpha]+\alpha[V_{\mathrm{PV}}(n)] \tag{1}$$

$$I_{\mathrm{PV\_filtered}}(n) = [I_{\mathrm{PV\_filtered}}(n-1)][1-\alpha]+\alpha[I_{\mathrm{PV}}(n)] \tag{2}$$

where the smoothing factor $\alpha = (\Delta T_s)/(\Delta T_s + \tau_c)$.

3) Calculate the PV array power using the filtered measured array signals

$$P_{\mathrm{PV}}(n) = V_{\mathrm{PV\_filtered}}(n) \times I_{\mathrm{PV\_filtered}}(n). \tag{3}$$

4) Calculate the change in the PV array power within 100 sample span (100 ΔT_s) for smoothing purpose

$$\Delta P_{\mathrm{PV}}(n) = P_{\mathrm{PV}}(n-100) - P_{\mathrm{PV}}(n). \tag{4}$$

The change in the array power is large at system startup and decreases until it reaches zero at steady state. The core of the proposed MPPT is to treat this power variation using a PI controller, as if it is an error that needs to be minimized, and utilize it to generate the perturb value for the array reference voltage. Hence, the perturbation is neither fixed nor user dependent, but adaptive as it is directly related to the system power variation.

5) Calculate the array reference voltage perturb value using a PI controller (perturb calculator discrete PI controller) for the system power variation

$$\begin{aligned}\Delta V^*_{\mathrm{PV}}(n) = {} & \Delta V^*_{\mathrm{PV}}(n-100) \\ & + K_{p\_\mathrm{perturb}}[\Delta P_{\mathrm{PV}}(n) - \Delta P_{\mathrm{PV}}(n-100)] \\ & + K_{i\_\mathrm{perturb}}\Delta T_s \Delta P_{\mathrm{PV}}(n)\end{aligned} \tag{5}$$

where K_{p_perturb} and K_{i_perturb} are the perturb calculator discrete PI controller proportional and integral constants, respectively. Note that for the limiter associated with the perturb calculator discrete PI controller, it is set to $\pm 10\%$ of the rated open-circuit voltage at standard insolation given in the PV array data sheet [46].

6) According to the P&O hill climbing algorithm, the array reference voltage perturb value is added/subtracted from the past array reference voltage based on the array voltage and current variations between the calculated instants (6), as shown at the bottom of the next page.
7) Calculate the error between the reference and the actual PV array voltage

$$e_{\mathrm{PV}}(n) = V^*_{\mathrm{PV}}(n) - V_{\mathrm{PV}}(n). \tag{7}$$

8) Generate the required converter duty ratio utilizing the second PI controller (boost converter discrete PI controller)

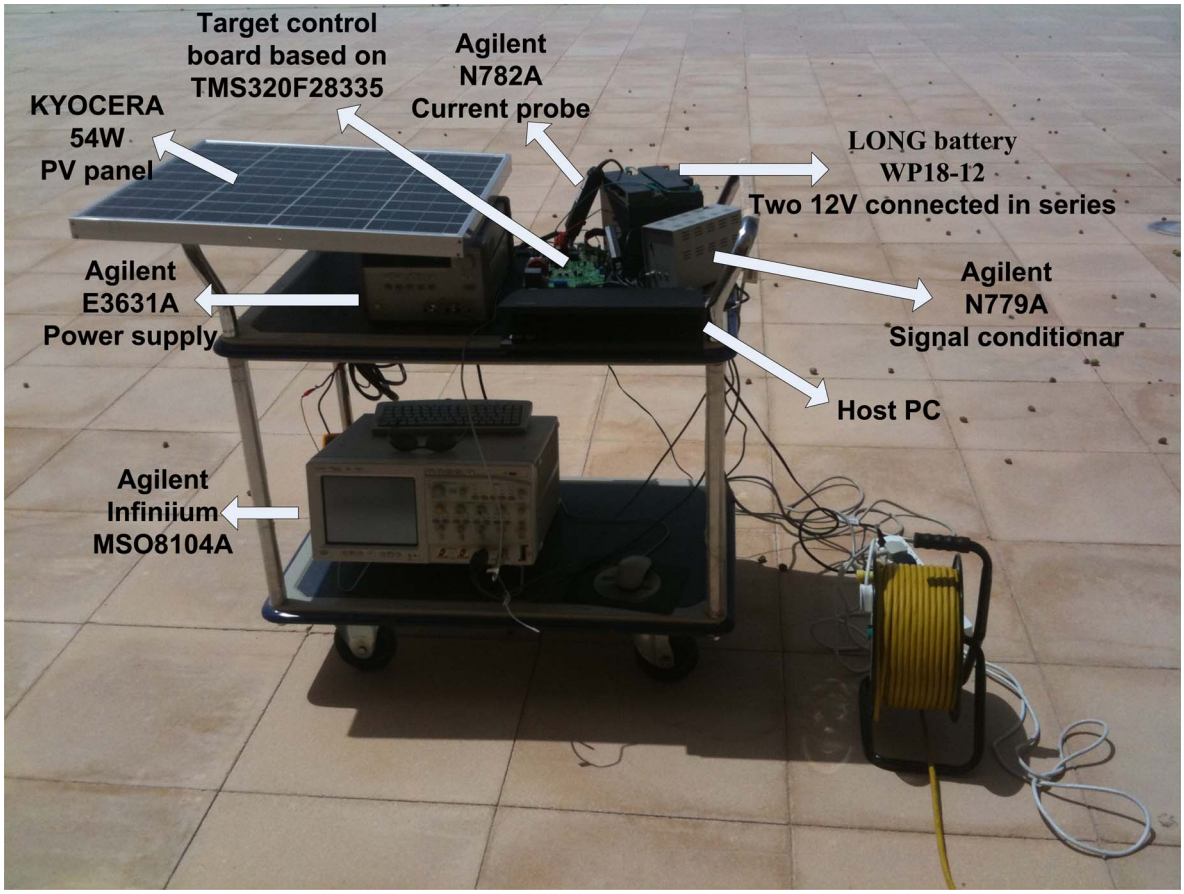

Fig. 4. Experimental test rig; Texas A&M University outdoor atrium.

$$d^*_{\rm boost}(n) = d^*_{\rm boost}(n-100) + K_{p\_{\rm boost}}[e_{\rm PV}(n) - e_{\rm PV}(n-100)] + K_{i\_{\rm boost}}\Delta T_s e_{\rm PV}(n) + \text{offset} \tag{8}$$

where $K_{p\_{\rm boost}}$ and $K_{i\_{\rm boost}}$ are the boost converter discrete PI controller proportional and integral constants, respectively, and $d^*_{\rm boost}$ is the boost converter duty ratio. Since the output from the boost converter discrete PI controller is ranging between $\pm$ limits, set to ± 50, an offset is needed to shift the calculated boost converter duty ratio to be in the level from 0% to 100% to suit the converter hardware.

C. Controller Tuning Steps

A cascaded controller tuning process is employed to operate the proposed technique. The tuning process is described as follows.

1) The P&O block is disabled by manually setting an arbitrary reference for the module voltage $V^*_{\rm PV}$. The perturb calculator discrete PI controller (responsible for generating the perturb value) is disabled in this way.
2) The boost converter discrete PI controller (responsible for generating converter duty cycle) is first tuned using an online Zigler–Nicholas method [45] as it represents the inner loop controller.
3) After achieving acceptable performance for the converter control, the next step starts by reenabling the P&O block.
4) The perturb calculator discrete PI controller is then tuned in a similar fashion, as in step 2, with the boost converter discrete PI controller treated as a unity gain.

IV. Experimental Setup and Results

In order to validate the proposed technique's effectiveness, a practical setup is arranged. Fig. 4 shows the details of the experimental setup. A 32-bit 150-MHz digital signal controller

$$V^*_{\rm PV}(n) = \begin{cases} V^*_{\rm PV}(n-100) - \Delta V^*_{\rm PV}(n), & [(P_{\rm PV}(n) > P_{\rm PV}(n-100)) \text{ AND } (V_{\rm PV}(n) < V_{\rm PV}(n-100))] \text{ OR} \\ & [(P_{\rm PV}(n) < P_{\rm PV}(n-100)) \text{ AND } (V_{\rm PV}(n) > V_{\rm PV}(n-100))] \\ V^*_{\rm PV}(n-100) + \Delta V^*_{\rm PV}(n), & [(P_{\rm PV}(n) > P_{\rm PV}(n-100)) \text{ AND } (V_{\rm PV}(n) > V_{\rm PV}(n-100))] \text{ OR} \\ & [(P_{\rm PV}(n) < P_{\rm PV}(n-100)) \text{ AND } (V_{\rm PV}(n) > V_{\rm PV}(n-100))] \end{cases}. \tag{6}$$

TABLE IV
EXPERIMENTAL SETUP COMPONENTS LIST

Element	*Manufacturer and part number*	*Value*
Inductor	Coilcraft DMT3-402-3.7L	402μH, 3.7A Toroidal power choke
Capacitor	-	3x1200μF, 35V electrolytic capacitors
Diode	ON semiconductors MUR405	50V, 4A ultrafast recovery diode
IGBT	International Rectifiers IRG4BC20UD	600V, 6.5A IGBT with ultrafast recovery diode
Load	LONG battery WP18-12	2x12V connected in series
PV array	KYOCERA KC50T	54W Solar panel

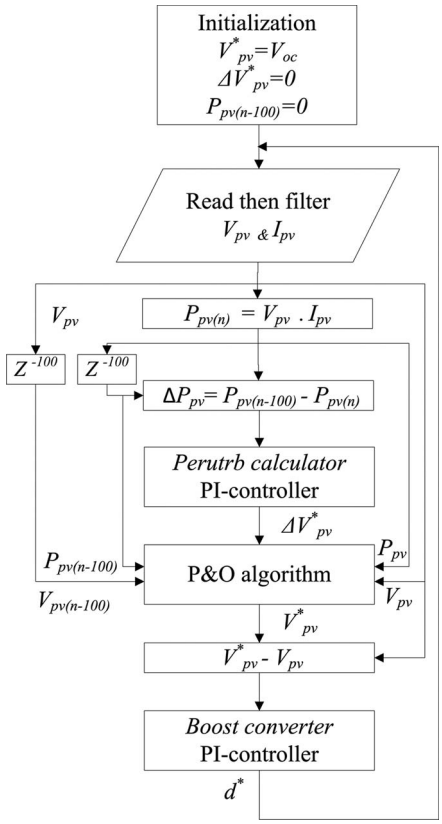

Fig. 5. Software flowchart.

TMS320F28335 is used as the main controller. The power circuit is basically a boost converter with parameters listed in Table IV.

The proposed PI–P&O technique is practically tested using the aforementioned setup, and compared with the conventional P&O technique with a fixed perturb. In order to achieve a full analysis for the system, the conventional P&O technique is tested with two values of perturb, one small and one large value. The test is carried in two outdoor environmental conditions, clear sunny and cloudy. The clear sunny condition presents high irradiance, while low irradiance is achieved by testing under cloudy conditions. The implemented software flowchart is illustrated in Fig. 5.

The test data are as follows.

1) Location: Texas A&M university outdoor atrium, Doha, Qatar.
2) Date: 20/4/2009.
3) Fig. 6 [Time: 1:30 P.M., temperature: 39.4 °C, irradiance: 900 W/m^2].
4) Fig. 7 [Time: 5:15 P.M., temperature: 28.3 °C, irradiance: 80 W/m^2].

It is noticed that the amplitude of oscillations in PV array power depends on the value of fixed perturb, as shown in parts (a) and (b) of Figs. 6 and 7. These power oscillations occur during MPPT using the fixed perturb, and are also directly proportional to perturb value. Power oscillations are a major source of losses as available PV power is not fully utilized. This trend is persistent despite of the irradiance and power level. From Figs. 6(c) and 7(c), the high-performance operation of the proposed PI–P&O technique is shown. Although the proposed technique relies on a relatively simple core, experimental results show improved performance and tracking compared to the fixed perturb technique. No oscillations around the MPP are achieved by the presented MPPT technique. Therefore, both system efficiency and tracking performance are enhanced. As a brief, the proposed technique is compared with all the previously mentioned adaptive techniques [34]–[40], as shown in Table V.

Although Figs. 6 and 7 show good performance of the proposed technique at steady state, the transient startup and sudden insolation change conditions need to be addressed. Hence, the proposed system is compared with the classical fixed perturb P&O technique with two different fixed perturb values 0.1 and 1 from transient point of view, considering startup and sudden insolation change, as shown in Fig. 8.

For the startup, nearly all the compared techniques possess the same performance if oscillations around steady-state value are disregarded, as shown in Fig. 8(a), (c), and (e).

The weather at the test rig location, Qatar, is not characterized by sudden insolation change as it is clear sunny nearly all over the year. Therefore, an artificial partial shadow is created on purpose by suddenly hiding a portion of the array using an opaque piece of paper. A very small difference, within milliseconds, in startup and sudden insolation change conditions is observed

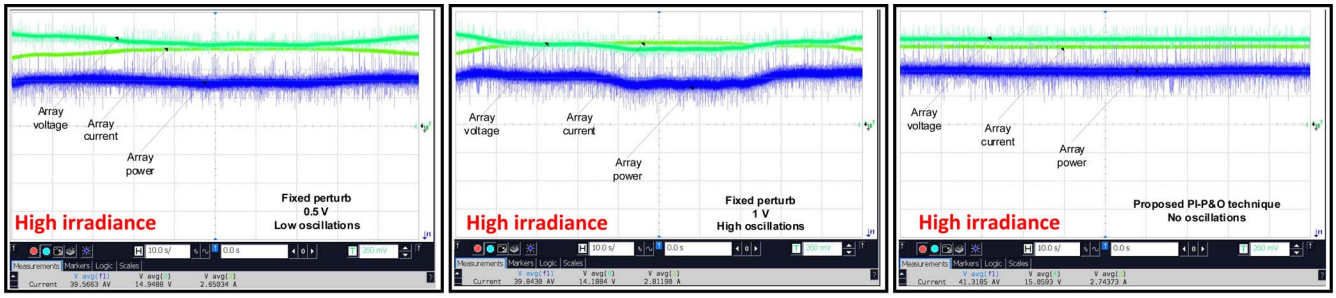

(a) (b) (c)

Fig. 6. Outdoor clear sunny condition (high irradiance) experimental results. (a) 0.5-V fixed perturb, (b) 1-V fixed perturb, and (c) proposed PI–P&O technique. Voltage scale: 5 V/div; current scale: 1 A/div; power scale: 20 W/div; and time scale: 10 s/div.

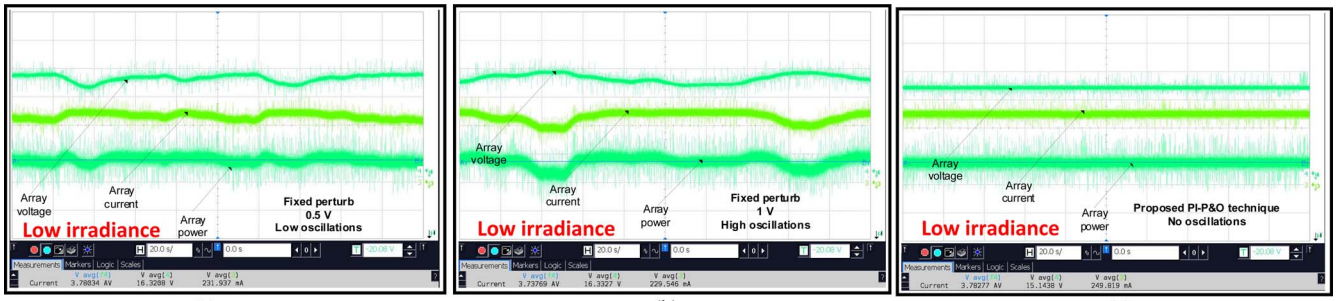

(a) (b) (c)

Fig. 7. Outdoor cloudy condition (low irradiance) experimental results. (a) 0.5-V fixed perturb, (b) 1-V fixed perturb, and (c) proposed PI–P&O technique. Voltage scale: 5 V/div; current scale: 0.1 A/div; power scale: 1 W/div; and time scale: 20 s/div.

TABLE V
COMPARISON BETWEEN THE PROPOSED PI–P&O TECHNIQUE AND OTHER ADAPTIVE P&O TECHNIQUES

P&O Techniques	*Perturb calculation*	*Is the technique a true adaptive?*	*Computational load complexity*	*Does the technique need system-dependant constants?*
A.al-amoudi *et al.* [34] and L. Zehang *et al.* [35]	Fixed discrete predetermined values, starts with 10% of the open circuit voltage and decreases by 50% till it saturates at 0.5% of the open circuit voltage	No	Minimal, Neither derivative nor division is required	Yes, the open circuit voltage needs to be initialized and updated continuously
H.Patel *et al.* [36]	Fixed discrete predetermined values, dependant on the power range (divided into four ranges)	No	Minimal, Neither derivative nor divisions is required	Yes, Perturb values are constants, system dependant and needs to be initialized before start-up
M. Chiang *et al* .[37]	$d(k) = d(k-1) \pm \frac{\lvert\Delta P/\Delta d\rvert}{\lvert P/d\rvert}$	Yes	High, One derivative and two divisions are needed	No, does not depend on any constants
W. Xiao *et al.* [38]	$d(k) = d(k-1) \pm \frac{M\lvert\Delta P\rvert}{d(k-1)}$	Yes	Low, No derivative is required but one division is needed	Yes, constant (M) needs to be initialized before start-up
P. Wolf *et al.*[39]	$d(k) = d(k-1) + M\frac{dP}{dV}$	Yes	Moderate, as it depends on derivative of power with respect to voltage	Yes, constant (M) needs to be initialized before start-up
A. Pandey *et al* .[40]	$d(k) = d(k-1) + M\frac{dP}{dV}$	Yes	High, due to derivative and simultaneous operation with FullCurve algorithm for rapidly changing weather detection	No, constant (M) is automatically calculated at start-up
Proposed	**Utilizes the change of array power as an error signal manipulated by a simple PI controller to generate an adaptive perturb**	**Yes**	**Minimal, Neither derivative nor division is required**	**No, but needs PI-controller tuning**

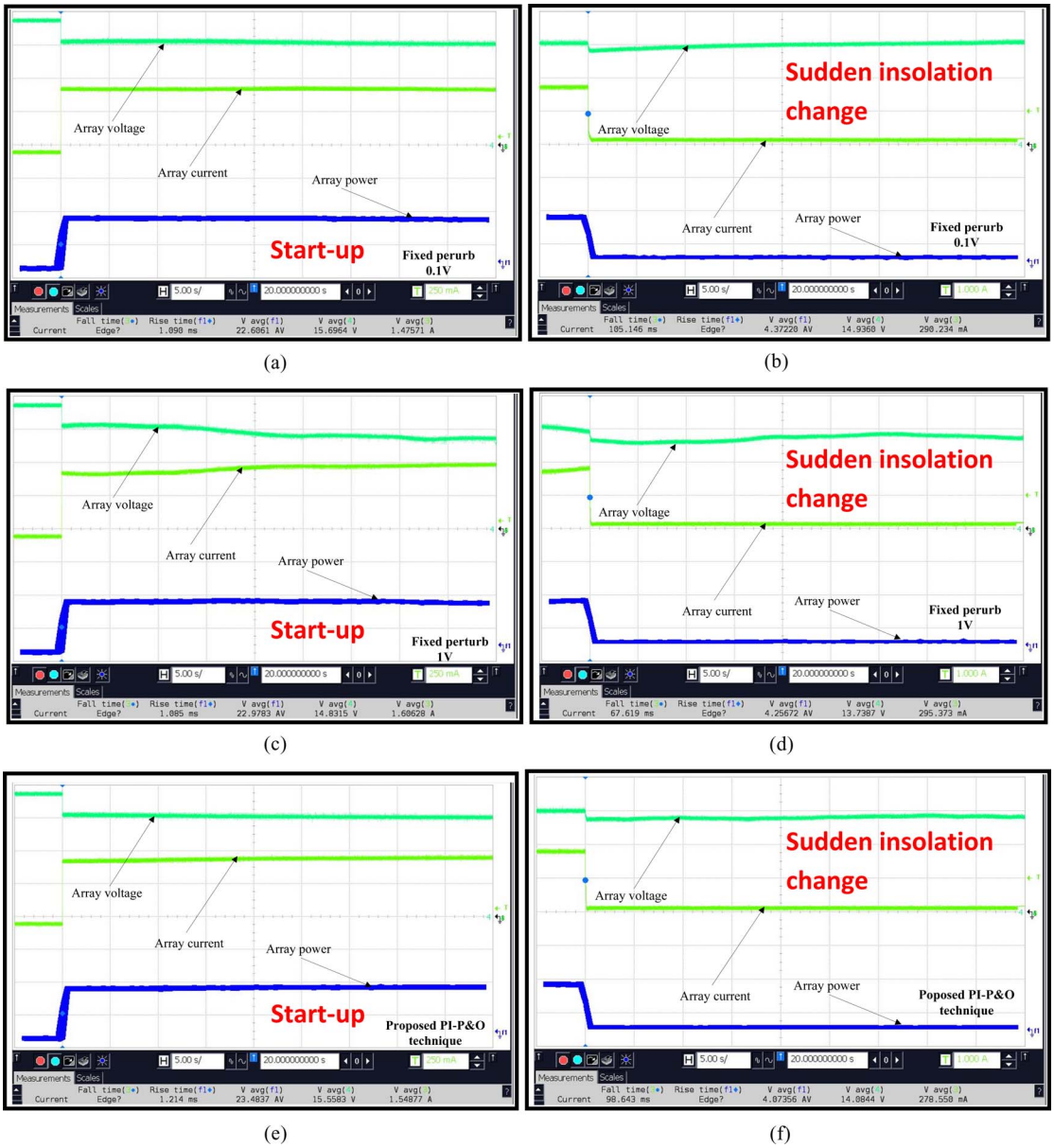

Fig. 8. Transient condition, startup and sudden insolation change, experimental results. (a) and (b) 0.5-V fixed perturb; (c) and (d) 1-V fixed perturb; and (e) and (f) proposed PI–P&O technique. Voltage scale: 5 V/div; current scale: 1 A/div and time scale: 5 s/div.

between the classical and the proposed technique revealing the fact that the main contribution of the proposed technique is basically in the steady state. The milliseconds time difference is negligible compared to the PV array time constant, which is in the range of tens of seconds, as shown in Figs. 6 and 7.

V. Conclusion

In this paper, a survey of P&O techniques has been presented. It has been shown that existing techniques suffer from oscillations, complexity, designer dependency, and high computational load. A modified P&O MPPT technique has been presented, which is suitable for a PV-based microgrids. The proposed technique, named PI–P&O, is generic, adaptive, and does not require any preset constants like other P&O techniques. It has been demonstrated that high-performance steady-state operation can be achieved with no oscillations around the MPP using the proposed technique. A comparison between the proposed technique and other adaptive P&O techniques has been carried out. Finally, an experimental setup has been held to demonstrate the capabilities of the proposed technique. Practical results for high- and low-irradiance conditions validate the proposed technique's effectiveness by comparing its performance to the fixed perturb technique.

References

[1] M. Barnes, J. Kondoh, H. Asano, J. Oyarzabal, G. Ventakaramanan, R. Lasseter, N. Hatziargyriou, and T. Green, "Real-world microgrids: An overview," in *Proc. IEEE Int. Conf. Syst. Syst. Eng.*, Apr. 16–18, 2007, pp. 1–8.

[2] J. M. Guerrero, F. Blaabjerg, T. Zhelev, K. Hemmes, E. Monmasson, S. Jemei, M. P. Comech, R. Granadino, and J. I. Frau, "Distributed generation: Toward a new energy paradigm," *IEEE Ind. Electron. Mag.*, vol. 4, no. 1, pp. 52–64, Mar. 2010.

[3] L. Zhang, S. Wang, Y. Zhao, and W. Tang, "Prospects for and applications to microgrid technology," in *Proc. Asia-Pacific Power Energy Eng. Conf.*, Mar. 28–31,, 2010, pp. 1–4.

[4] M. Liserre, T. Sauter, and J. Y. Hung, "Future energy systems: Integrating renewable energy sources into the smart power grid through industrial electronics," *IEEE Ind. Electron. Mag.*, vol. 4, no. 1, pp. 18–37, Mar. 2010.

[5] T. Esram and P. L. Chapman, "Comparison of photovoltaic array maximum power point tracking techniques," *IEEE Trans. Energy Conv.*, vol. 22, no. 2, pp. 439–449, Jun. 2007.

[6] S. Jain and V. Agarwal, "Comparison of the performance of maximum power point tracking schemes applied to single-stage grid-connected photovoltaic systems," *IET Electr. Power Appl.*, vol. 1, no. 5, pp. 753–762, Sep. 2007.

[7] H. P. Desai and H. K. Patel, "Maximum power point algorithm in PV generation: An overview," in *Proc. 7th Int. Conf. Power Electron. Drive Syst.*, Nov. 27–30, 2007, pp. 624–630.

[8] M. G. Villalva, J. R. Gazoli, and E. R. Filho, "Comprehensive approach to modeling and simulation of photovoltaic arrays," *IEEE Trans. Power Electron.*, vol. 24, no. 5, pp. 1198–1208, May 2009.

[9] Q. Li and P. Wolfs, "A review of the single phase photovoltaic module integrated converter topologies with three different DC link configurations," *IEEE Trans. Power Electron.*, vol. 23, no. 3, pp. 1320–1333, May 2008.

[10] T. Kerekes, M. Liserre, R. Teodorescu, C. Klumpner, and M. Sumner, "Evaluation of three-phase transformerless photovoltaic inverter topologies," *IEEE Trans. Power Electron.*, vol. 24, no. 9, pp. 2202–2211, Sep. 2009.

[11] O. Wasynezuk, "Dynamic behavior of a class of photovoltaic power systems," *IEEE Trans. Power Apparatus Syst.*, vol. PAS-102, no. 9, pp. 3031–3037, Sep. 1983.

[12] W. J. A. Teulings, J. C. Marpinard, A. Capel, and D. O'Sullivan, "A new maximum power point tracking system," *Conf. Rec. 24th Annu. IEEE Power Electron. Spec. Conf.*, pp. 833–838, Jun. 20–24, 1993.

[13] C. Hua and J. R. Lin, "DSP-based controller application in battery storage of photovoltaic system," in *Proc. IEEE IECON 22nd Int. Conf. Ind. Electron., Control, Instrum.*, Aug. 5–10, 1996, vol. 3, pp. 1705–1710.

[14] Y. Kim, H. Jo, and D. Kim, "A new peak power tracker for cost-effective photovoltaic power system," in *Proc. 31st Intersoc. Energy Conv. Eng. Conf.*, Aug. 11–16,, 1996, vol. 3, pp. 1673–1678.

[15] Y. Jung, G. Yu, J. Choi, and J. Choi, "High-frequency DC link inverter for grid-connected photovoltaic system," *Conf. Rec. 29th IEEE Photovoltaic Spec. Conf.*, pp. 1410–1413, May 19–24, 2002.

[16] K. Chomsuwan, P. Prisuwanna, and V. Monyakul, "Photovoltaic grid-connected inverter using two-switch buck-boost converter," *Conf. Rec. 29th IEEE Photovoltaic Spec. Conf.*, pp. 1527–1530, May 19–24, 2002.

[17] T. Shimizu, O. Hashimoto, and G. Kimura, "A novel high-performance utility-interactive photovoltaic inverter system," *IEEE Trans. Power Electron.*, vol. 18, no. 2, pp. 704–711, Mar. 2003.

[18] N. Femia, G. Lisi, G. Petrone, G. Spagnuolo, and M. Vitelli, "Distributed maximum power point tracking of photovoltaic arrays: Novel approach and system analysis," *IEEE Trans. Ind. Electron.*, vol. 55, no. 7, pp. 2610–2621, Jul. 2008.

[19] M. Fortunato, A. Giustiniani, G. Petrone, G. Spagnuolo, and M. Vitelli, "Maximum power point tracking in a one-cycle-controlled single-stage photovoltaic inverter," *IEEE Trans. Ind. Electron.*, vol. 55, no. 7, pp. 2684–2693, Jul. 2008.

[20] E. Figueres, G. Garcera, J. Sandia, F. Gonzalez-Espin, and J. C. Rubio, "Sensitivity study of the dynamics of three-phase photovoltaic inverters with an LCL grid filter," *IEEE Trans. Ind. Electron.*, vol. 56, no. 3, pp. 706–717, Mar. 2009.

[21] H. Patel and V. Agarwal, "Investigations into the performance of photovoltaics-based active filter configurations and their control schemes under uniform and non-uniform radiation conditions," *IET Renewable Power Gener.*, vol. 4, no. 1, pp. 12–22, Jan. 2010.

[22] S.-H. Park, G.-R. Cha, Y.-C. Jung, and C.-Y. Won, "Design and application for PV generation system using a soft-switching boost converter with SARC," *IEEE Trans. Ind. Electron.*, vol. 57, no. 2, pp. 515–522, Feb. 2010.

[23] M. A. Slonim and L. M. Rahovich, "Maximum power point regulator for 4 kW solar cell array connected through invertor to the AC grid," in *Proc. 31st Intersoc. Energy Conv. Eng. Conf.*, Aug. 11–16, 1996, vol. 3, pp. 1669–1672.

[24] N. Kasa, T. Lida, and H. Iwamoto, "Maximum power point tracking with capacitor identifier for photovoltaic power system," in *IEE Proc. Elect. Power Appl.*, Nov. 2000, vol. 147, no. 6, pp. 497–502.

[25] E. Koutroulis, K. Kalaitzakis, and N. C. Voulgaris, "Development of a microcontroller-based, photovoltaic maximum power point tracking control system," *IEEE Trans. Power Electron.*, vol. 16, no. 1, pp. 46–54, Jan. 2001.

[26] M. Veerachary, T. Senjyu, and K. Uezato, "Maximum power point tracking control of IDB converter supplied PV system," in *IEE Proc. Electric Power Appl.*, Nov. 2001, vol. 148, no. 6, pp. 494–502.

[27] Y.-T. Hsiao and C.-H. Chen, "Maximum power tracking for photovoltaic power system," in *Conf. Rec. 37th IAS Annu. Meeting Ind. Appl. Conf.*, 2002, vol. 2, pp. 1035–1040.

[28] N. Kasa, T. Iida, and L. Chen, "Flyback inverter controlled by sensorless current MPPT for photovoltaic power system," *IEEE Trans. Ind. Electron.*, vol. 52, no. 4, pp. 1145–1152, Aug. 2005.

[29] S. Jain and V. Agarwal, "A single-stage grid connected inverter topology for solar PV systems with maximum power point tracking," *IEEE Trans. Power Electron.*, vol. 22, no. 5, pp. 1928–1940, Sep. 2007.

[30] R. Gules, J. De Pellegrin Pacheco, H. L. Hey, and J. Imhoff, "A maximum power point tracking system with parallel connection for PV stand-alone applications," *IEEE Trans. Ind. Electron.*, vol. 55, no. 7, pp. 2674–2683, Jul. 2008.

[31] J.-M. Kwon, B.-H. Kwon, and K.-H. Nam, "Three-phase photovoltaic system with three-level boosting MPPT control," *IEEE Trans. Power Electron.*, vol. 23, no. 5, pp. 2319–2327, Sep. 2008.

[32] J.-M. Kwon, B.-H. Kwon, and K.-H. Nam, "Grid-connected photovoltaic multistring PCS with PV current variation reduction control," *IEEE Trans. Ind. Electron.*, vol. 56, no. 11, pp. 4381–4388, Nov. 2009.

[33] C. Liu, K. T. Chau, and X. Zhang, "An efficient wind–photovoltaic hybrid generation system using doubly excited permanent-magnet brushless machine," *IEEE Trans. Ind. Electron.*, vol. 57, no. 3, pp. 831–839, Mar. 2010.

[34] A. Al-Amoudi and L. Zhang, "Optimal control of a grid-connected PV system for maximum power point tracking and unity power factor," in *Proc. 7th Int. Conf. Power Electron. Variable Speed Drives (Conf. Publ. No. 456)*, Sep. 21–23,, 1998, pp. 80–85.

[35] L. Zhang, A. Al-Amoudi, and Y. Bai, "Real-time maximum power point tracking for grid-connected photovoltaic systems," in *Proc. 8th Int. Conf. Power Electron. Variable Speed Drives (IEE Conf. Publ. No. 475)*, 2000, pp. 124–129.

[36] H. Patel and V. Agarwal, "MPPT Scheme for a PV-fed single-phase single-stage grid-connected inverter operating in CCM with only one current sensor," *IEEE Trans. Energy Convers.*, vol. 24, no. 1, pp. 256–263, Mar. 2009.

[37] M.-L. Chiang, C.-C. Hua, and J.-R. Lin, "Direct power control for distributed PV power system," in *Proc. Power Convers. Conf.*, Osaka, Japan, 2002, pp. 311–315.

[38] W. Xiao and W. G. Dunford, "A modified adaptive hill climbing MPPT method for photovoltaic power systems," in *Proc. IEEE 35th Annu. Power Electron. Spec. Conf.*, Jun. 20–25, 2004, vol. 3, pp. 1957–1963.

[39] P. J. Wolfs and L. Tang, "A single cell maximum power point tracking converter without a current sensor for high performance vehicle solar arrays," in *Proc. IEEE 36th Power Electron. Spec. Conf.*, Jun. 16–16, 2005, pp. 165–171.

[40] A. Pandey, N. Dasgupta, and A. K. Mukerjee, "High-performance algorithms for drift avoidance and fast tracking in solar MPPT system," *IEEE Trans. Energy Convers.*, vol. 23, no. 2, pp. 681–689, Jun. 2008.

[41] S. Jain and V. Agarwal, "A new algorithm for rapid tracking of approximate maximum power point in photovoltaic systems," *IEEE Power Electron. Lett.*, vol. 2, no. 1, pp. 16–19, Mar. 2004.

[42] N. S. D'Souza, L. A. C. Lopes, and X. Liu, "An intelligent maximum power point tracker using peak current control," in *Proc. IEEE 36th Power Electron. Spec. Conf.*, Jun. 16–16, 2005, pp. 172–177.

[43] N. Femia, G. Petrone, G. Spagnuolo, and M. Vitelli, "Optimization of perturb and observe maximum power point tracking method," *IEEE Trans. Power Electron.*, vol. 20, no. 4, pp. 963–973, Jul. 2005.

[44] N. Femia, G. Petrone, G. Spagnuolo, and M. Vitelli, "A technique for improving P&O MPPT performances of double-stage grid-connected photovoltaic systems," *IEEE Trans. Ind. Electron.*, vol. 56, no. 11, pp. 4473–4482, Nov. 2009.

[45] K. Astrom and T. Hagglund, *PID Controllers: Theory, Design, and Tuning*, NC: International Society for Measurement and Control, 1995.

[46] Kyocera. [Online]. (accessed June 2010) Available http://www.kyocerasolar.com/pdf/specsheets/KC50T.pdf.

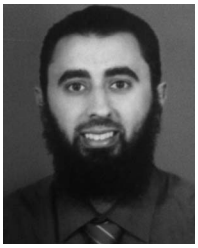

Ahmed K. Abdelsalam (M'10) received the B.Sc. and M.Sc. degrees from the Faculty of Engineering, Alexandria University, Alexandria, Egypt, in 2002 and 2006, respectively, and the Ph.D. degree in electrical engineering from the Department of Electrical and Electronic Engineering, Strathclyde University, Glasgow, U.K., in 2009.

Since 2010, he has been with Texas A&M University at Qatar, Doha, Qatar, where he is currently a Postdoctoral Research Associate in the Department of Electrical and Computer Engineering. His research interests include motor drives, power quality, distributed generation, and power converters for renewable energy systems.

Dr. Abdelsalam is a member of the IEEE Power Electronics and IEEE Industrial Electronics societies, and the Institute of Engineering and Technology.

Ahmed M. Massoud (M'10) received the B.Sc. (first class honors) and M.Sc. degrees from the Faculty of Engineering, Alexandria University, Alexandria, Egypt, in 1997 and 2000, respectively, and the Ph.D. degree in electrical engineering from the Computing and Electrical Department, Heriot-Watt University, Edinburgh, U.K., in 2004.

From 2005 to 2008, he was a Research Fellow at Strathclyde University, Glasgow, U.K. From 2008 to 2009, he was a Research Fellow at Texas A&M at Qatar, Doha, Qatar. He is currently an Assistant Professor at the Department of Electrical Engineering, Faculty of Engineering, Qatar University, Doha. His research interests include power quality, active power filtering, distributed generation, and multilevel converters.

Shehab Ahmed (M'07) received the B.Sc. degree in electrical engineering from Alexandria University, Alexandria, Egypt, in 1999, and the M.Sc. and Ph.D. degrees from the Department of Electrical Engineering, Texas A&M University, College Station, in 2000 and 2007, respectively.

From 2001 to 2007, he was with Schlumberger Technology Corporation, where he was engaged in research on downhole mechatronic systems. He is currently an Assistant professor at Texas A&M University at Qatar, Doha, Qatar. His research interests include mechatronics, solid-state power conversion, electric machines, and drives.

Prasad N. Enjeti (M'85–SM'95–F'00) received the B.E. degree in electrical engineering from Osmania University, Hyderabad, India, in 1980, the M.Tech. degree in electrical engineering from the Indian Institute of Technology Kanpur, Kanpur, India, in 1982, and the Ph.D. degree in electrical engineering from Concordia University, Montreal, QC, Canada, in 1988.

In 1988, he joined the Department of Electrical Engineering, Texas A&M University, College Station, as an Assistant Professor, where he became an Associate Professor in 1994, a Full Professor in 1998, and is currently the Lead Developer of the Power Electronics/Power Quality and Fuel Cell Power Conditioning Laboratories. He is actively involved in many projects with industries, while engaged in teaching, research, and consulting in the area of power electronics, motor drives, power quality, and clean power utility interface issues. He is the holder of four U.S. patents and has licensed two new technologies to the industry so far. His current research interests include advanced converters for power supplies and motor drives, power quality issues, active power filter development, utility interface issues, advancing switching power supply designs and solutions to complex power management issues in the context of analog and mixed-signal applications, exploring alternative designs to meet the demands of high slew-rate load currents at low output voltages, power conditioning systems for fuel cells, wind, and solar energy systems, and design of high-temperature power conversion systems with wideband gap semiconductor devices.